Influence of silver nanoparticles and liberated silver ions on nitrifying sludge: ammonia oxidation inhibitory kinetics and mechanism

Nguyen Thanh Giao[1,2] · Tawan Limpiyakorn[2,3,4] · Pattaraporn Kunapongkiti[2,3] · Pumis Thuptimdang[5] · Sumana Siripattanakul-Ratpukdi[1,2,6]

Abstract Silver nanoparticles (AgNPs) are widely used in commercial products because of their excellent antimicrobial activity. Entrance of AgNPs and its released Ag ions (Ag$^+$) into wastewater treatment plants could harm ammonia oxidation (AO) process resulting in environmental problems. This study investigated inhibitory kinetics and mechanism of AO from nitrifying sludge influenced by AgNPs and Ag$^+$. The findings demonstrated that AgNPs and Ag$^+$ adversely influenced on AO. Silver ions were more toxic to AO than AgNPs, which was indicated by the lower inhibitory constant (K_i) of 0.29 mg/L compared to that of AgNPs (K_i of 73.5 mg/L). Over the experimental period of 60 h, AgNPs at 1, 10, and 100 mg/L released Ag$^+$ in the average concentrations of 0.059, 0.171, and 0.503 mg/L, respectively. Silver nanoparticles of 1– 100 mg/L inhibited AO by 45–74%, whereas Ag$^+$ of 0.05– 0.50 mg/L inhibited AO by 53–94%. This suggested that the AgNP toxicity mainly derived from the liberated Ag$^+$. Scanning electron microscopy results revealed that AgNPs attached on microbial cell surfaces, and both AgNPs and Ag$^+$ induced cell morphological change from rod shape to shorter rod shape. Transmission electron microscopy showed that AgNPs and Ag$^+$ diminished the thickness of the outer layer and reduced the density of internal parts of the exposed microbial cells, which could be the reasons for the morphology change. Live/dead results also confirmed that AgNPs and Ag$^+$ damaged membrane integrity of cells in the nitrifying sludge. This study suggested that the primary mechanism for toxicity of AgNPs was the liberation of Ag$^+$ and then both of silver species caused cell death.

Keywords AgNPs · Ammonia oxidation · Inhibitory kinetics · Nanosilver · Nitrifying sludge · Silver ions

✉ Sumana Siripattanakul-Ratpukdi
  sumana.r@kku.ac.th; jeans_sumana@yahoo.com

1 International Program in Hazardous Substance and Environmental Management, Graduate School, Chulalongkorn University, Bangkok 10330, Thailand

2 Research Program in Hazardous Substance Management in Agricultural Industry, Center of Excellence on Hazardous Substance Management, Bangkok 10330, Thailand

3 Department of Environmental Engineering, Faculty of Engineering, Chulalongkorn University, Bangkok 10330, Thailand

4 Research Unit Control of Emerging Micropollutants in Environment, Chulalongkorn University, Bangkok 10330, Thailand

5 Department of Environmental Science, School of Energy and Environment, University of Phayao, Phayao 56000, Thailand

6 Department of Environmental Engineering, Faculty of Engineering and Research Center for Environmental and Hazardous Substance Management, Khon Kaen University, Khon Kaen 40002, Thailand

Introduction

Silver nanoparticles (AgNPs) are extensively used in many consumer and medical products due to its high surface area and excellent antimicrobial activity (Massarsky et al. 2014). With increasing production and use, AgNPs were expected to be washed out from consumer products and unavoidably occurred in wastewater treatment plants (WWTPs) (Choi et al. 2009; Gu et al. 2014; Westerhoff et al. 2013). For instance, it was reported that 190 to 410 t of silver used in global textile and plastic industries were annually released to wastewater treatment systems (Siripattanakul-Ratpukdi and Fürhacker 2014). Former studies showed that silver was detected ranging from 4 μg/L to 1 mg/L and 2 to 195 mg/L in the influent concentration and biosolid concentration of WWTP,

respectively (Schildkraut et al. 1998; Shafer et al. 1998; USEPA 2009).

Since silver is classified as a highly toxic, persistent, and accumulated chemical, the performance of WWTPs may be adversely impacted due to the interactions between AgNPs and activated sludge (Gu et al. 2014; Siripattanakul-Ratpukdi et al. 2014). Nitrification process is known as the most sensitive process in WWTPs. The nitrification process includes ammonia oxidation (AO) and nitrite oxidation reactions. This AO, which was the rate-limiting step of the process, was previously found susceptible to AgNPs (Choi et al. 2008; Gu et al. 2014; Yang et al. 2013). Silver speciation related to AgNPs included AgNPs themselves and released silver ions (Ag^+). During AgNP oxidation, reactive oxygen species (ROS) could be created (Li et al. 2015; Massarsky et al. 2014; Yuan et al. 2013). Prior studies discovered that both AgNPs and Ag^+ clearly affected a wide range of organisms including nitrifying microbes (Choi et al. 2008; Yang et al. 2014). Among previous works, roles of AgNPs or the released Ag^+ to overall toxicity of AgNPs suspension were found differently due to varying experimental conditions including tested conditions, types of AgNPs, and nitrifying cultures. This inconclusive phenomenon was inadequate to finalize environmental treatment technology and management.

The aim of this study was to determine influence of silver species related to AgNPs on AO process. Inhibitory kinetics and mechanism of AO activity were investigated. Observation of microbial cell physiology, community, and viability using microscopic techniques including scanning electron microscopy (SEM), transmission electron microscopy (TEM), and confocal laser scanning microscopy (CLSM) was carried out. The result from this study can be used as the fundamental information for WWTP design and operation later on.

Materials and methods

Source of AgNPs and Ag^+

Silver nanoparticles (5000 mg/L) were purchased from PrimeNANO technology (Prime Nanotechnology Co. Ltd., Chulalongkorn University, Thailand). It was chemically synthesized from silver nitrate ($AgNO_3$) using sodium borohydride ($NaBH_4$) and starch as the reducing and capping agents, respectively. The AgNPs were in spherical shapes and the sizes were in the range of 2–12 nm, which were confirmed by TEM (Fig. 1). The localized surface plasmon resonance (LSPR) of AgNP suspensions (1–40 mg/L, prepared in SWW) was characterized using spectrophotometric technique at wavelengths of 250–600 nm (UV-Visible Spectrophotometer Biomate 3S, Thermo Scientific, WI, USA). It was indicated that AgNPs were well-dispersed form with nanosizes and since AgNPs suspension peaked at absorbance

spectrum (λ_{max}) of 400 nm. In addition, the initial Ag^+ in stock solution of AgNPs at 100 mg/L (prepared in distilled water) was found to be less than detection limit (3 μg/L). Silver nitrate ($AgNO_3$, Merck, Darmstadt, Germany) was used as source of Ag^+.

Nitrifying sludge

Seed sludge was taken from a continuous flow nitrifying culture-enriching reactor. The reactor has been operating with both hydraulic retention (HRT) and solid retention time (SRT) of 4 days with no sludge return. The collected seed sludge was then cultivated in a batch reactor, at room temperature (28–30 °C), with HRT and SRT of 14 days, at initial NH_4^+–N concentration of 429 ± 62 mg N/L. The dissolved oxygen (DO) concentration was maintained above 2 mg/L, and pH was adjusted between 7.0 and 7.8 using 5 N NaOH. The batch reactor fed with inorganic synthetic wastewater (SWW).

The composition of SWW contained 1.8877 g/L $(NH_4)_2SO_4$, 0.2 g/L NaCl, 0.2 g/L K_2HPO_4, 0.4 g/L $MgCl_2$·$6H_2O$, 0.1 g/L $CaCl_2$·$2H_2O$, 0.5 g/L KCl, and 1 g/L $NaHCO_3$ with an addition of inorganic salt solution (1 mL). The inorganic salt solution comprised of 40 g/L $MgSO_4$ $7H_2O$, 40 g/L $CaCl_2$ $2H_2O$, 200 g/L KH_2PO_4, 1 g/L $FeSO_4$ $7H_2O$, 0.1 g/L Na_2MoO_4, 0.2 g/L $MnCl_2$ $4H_2O$, 0.02 g/L $CuSO_4$ $5H_2O$, 0.1 g/L $ZnSO_4$ $7H_2O$, and 0.002 g/L $CoCl_2$ $6H_2O$. For the kinetic experiments, the synthetic wastewater was followed (Gu et al. 2014). The composition of wastewater was comprised of $(NH_4)_2SO_4$, 1 g/L $NaHCO_3$, 0.1 g/L K_2HPO_4, 0.025 g/L $MgSO_4$, and 0.025 g/L NaCl with AgNPs and Ag^+ at different concentrations.

Inhibitory kinetics and mechanism of ammonia oxidation

Inhibitory kinetics experiments The nitrifying sludge was harvested and centrifuged at 5000 rpm for 20 min, and the clear supernatant was removed to collect the settled cells. The collected cells were resuspended in SWW and washed by centrifugal process. The washing process was repeated for five times to obtain the cleaned cells, which were later used for the inhibitory kinetics tests. The ammonia oxidation kinetic experiments were carried out for the period of 60 h using 250-mL flask with an effective volume of 100 mL. The final biomass concentration was 50 mg/L as mixed liquored suspended solid (MLSS). All tests were conducted in triplicates at DO >2 mg/L and room temperature (28–30 °C) in batch mode. The pH of the neutral range (7.5–7.8) was achieved using 30 mM of HEPES. The initial NH_4^+–N concentrations were in the range of 0.85 to 73 mg/L and 0.9 to 260 mg/L for AgNPs and Ag^+ experiments, respectively. The final AgNP and Ag^+ concentrations were 1, 10, and 100 mg/L and 0.05, 0.10, 0.50, and 5.00 mg/L, respectively. It is noted that the Ag^+ concentrations were selected based on released
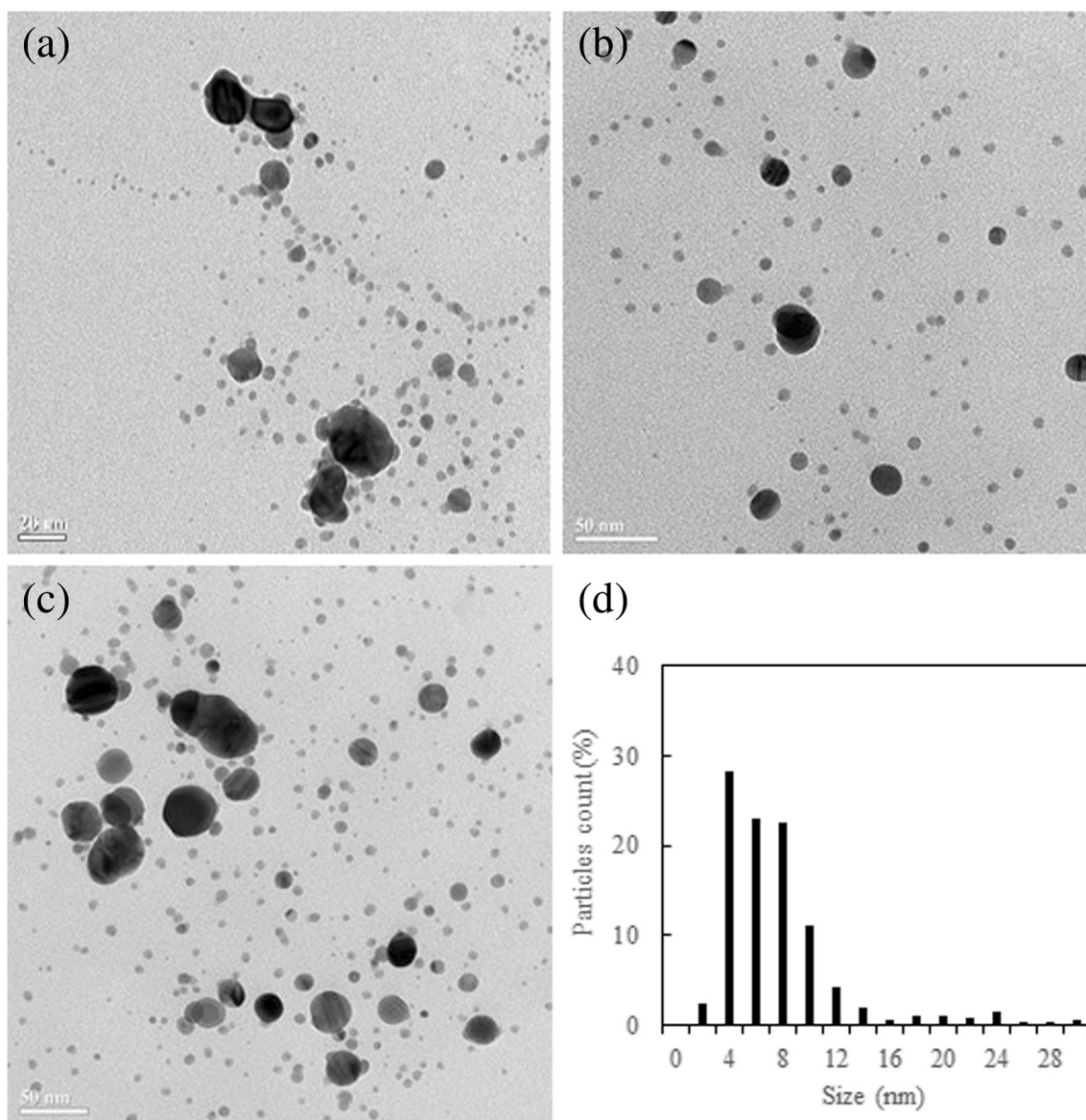
Fig. 1 TEM of AgNPs (**a–c**) and percent of particles count (**d**)

Ag$^+$ from AgNPs. Quantification of Ag$^+$ concentrations followed a previous method by Beer et al. (2012) (description of the method is shown in later subsection). The selected concentrations of Ag$^+$ based on the released Ag$^+$ result were discussed in the "Results and discussion" section.

The aqueous samples of 5 mL were collected periodically at 0, 3, 6, 9, 30, and 60 h to measure reduction of NH$_4^+$–N and production of nitrate (NO$_3^-$–N). The NH$_4^+$–N concentration was measured by salicylate–hypochlorite method (Bower and Holm-Hansen 1980) whereas the nitrite (NO$_2^-$–N) plus NO$_3^-$–N addressed by total NO$_2^-$–N was measured by colorimetric method 4500 (APHA 1998) after NO$_3^-$–N in aqueous samples were converted to NO$_2^-$–N by using vanadium chloride (VCl$_3$, 0.8 g in 100 ml HCl 1 M). The data from the experiment were used to calculate the kinetic values and inhibition percentage.

Silver ion release monitoring Silver ion release monitoring experiments were performed with the AgNP concentrations of 1, 10, and 100 mg/L and initial NH$_4^+$–N concentrations of 20 and 100 mg/L. The aqueous samples were collected at 0, 30, and 60 h. Approximate 8 mL of each aqueous sample was transferred into an ultracentrifuge tube (16 × 57 mm, Beckman Coulter, Inc., USA) and tightly sealed. The prepared samples were placed in ultracentrifuge machine (Optima™ MAX-XP Ultracentrifuge, Beckman Coulter, Inc., USA) and centrifuged at 165000×g, 4 °C, for 2 h (Beer et al. 2012) using MLN-80 rotor (16 × 58 mm, Beckman Coulter, Inc., USA). The centrifuged samples were carefully taken out, and the supernatants were gently withdrawn using 10-mL sterile syringes and transferred to glass bottles. The supernatants were sent to analyze at the certified laboratory at the Scientific and Technology Research Equipment Center (STREC,

Chulalongkorn University, Thailand) using Atomic Absorbance Spectrometry (AAS, Varian Model AA280FS, Australia). The measurement of total silver in the AAS was done using air/acetylene flame type with the air and acetylene flow rates of 13.6 and 1.80 L/min, respectively. The absorbance of silver was detected at the wavelength of 328.1 nm for 4.5 s. The detection limit of AAS was 3 µg Ag/L.

Kinetics calculation The NH_4^+–N oxidation rate was calculated according to Eq. 1 by comparing the change of NH_4^+–N reduction versus time, whereas the kinetic parameters including maximum NH_4^+–N oxidation rate (q_{max}) and half-saturation constant (K_s) were calculated from the Monod equation in Eq. 2.

$$q = \frac{dS}{dt} \tag{1}$$

$$q = \frac{q_{max}S}{K_s + S} \tag{2}$$

where q is the NH_4^+–N oxidation rate (mg N/L/h), q_{max} is the maximum NH_4^+–N oxidation rate (mg N/L/h), S is the initial NH_4^+–N concentration (mg/L), K_s is the half-saturation constant for ammonia (mg N/L), t is the time (h). Under the presence of AgNPs or Ag^+, Eq. 2 can be modified as shown in Eq. 3.

$$q = \frac{\left(q_{max} / \left(1 + \frac{I}{K_i}\right)\right)S}{K_s / \left(1 + \frac{I}{K_i}\right) + S} \tag{3}$$

where K_i is the inhibitory constant (mg AgNPs/L or mg Ag^+/L), and i can be AgNPs or Ag^+. The level of toxicity of a substance to a target microorganism can be indicated by the K_i value in which a higher toxicity level would be represented by a lower K_i value.

Inhibition calculation The percentage of inhibition of AO activity was calculated based on Eq. 4, which compares the rates of AO in the controls and in the AgNPs or Ag^+ treatments.

$$\text{Inhibition}\,(\%) = \frac{(q_c - q_i) \times 100}{q_c} \tag{4}$$

where q_c is the NH_4^+–N oxidation rate in the controls (mg N/L/h), q_i is the NH_4^+–N oxidation rate under the presence of AgNPs or Ag^+ (mg N/L/h). The percentage of inhibition caused by AgNPs and Ag^+ was presented as an averaged percent inhibition (%) ± standard deviation (SD) regardless of the initial NH_4^+–N concentrations. Statistical comparison was performed using IBM SPSS statistics for Windows, version 19.0 (IBM Corp., Armonk, NY, USA). The significance of the differences ($P < 0.05$) was determined by the analysis of

one-way analysis of variance (ANOVA) followed by Duncan's test (Ahrari et al. 2015).

Microbial cell physiology, community, and viability observation

Scanning electron microscopy observation The nitrifying sludge samples from the control test and the AgNPs and Ag^+-exposed tests were centrifuged at 5000 rpm for 5 min at 4 °C to remove the supernatant. The centrifuged samples were rinsed with phosphate buffer solution (PBS, 0.1 M, pH 7.4). The phosphate buffer solution was used because it can maintain osmotic balance between inside and outside of cells. The washed samples were fixed by using 0.1 M PBS with 4% glutaraldehyde overnight at 4 °C. The fixed samples were separated in half in liquid nitrogen, dehydrated using a series of ethanol solutions, placed on a stub, and covered with gold under vacuum condition. The prepared samples were examined using SEM (JEOL, JSM-5410LV, Tokyo, Japan), and the elemental compositions of selected areas were analyzed using energy-dispersive X-ray (EDX, Oxford Instruments, Model X-Max[N], UK).

Transmission electron microscopy observation The nitrifying sludge samples from the control test and the AgNPs and Ag^+-exposed tests were centrifuged at 5000 rpm for 5 min at 4 °C to remove the supernatant. The clean pellets were obtained by washing with NaCl of 0.85%. This concentration of NaCl was in the same range compared to one used in SWW. Also, the salt concentration is recommended for cleaning cells in another related kit (LIVE/DEAD® BacLight™ Bacterial Viability, Molecular Probes, Invitrogen). The additional damage of cells due to washing process was not expected. The washed samples were fixed with a glutaraldehyde solution of 2.5%. The fixed cells were washed in phosphate buffer and a 1% osmium tetroxide solution. The cells were mixed with 1.5% of the melt agar to form gel at 45–50 °C. The hardened agar was cut into 0.5-mm cubes. The cubes with cells were dehydrated with a series of ethanol solution from 35 to 95% (v/v). The dehydrated cubes were saturated in a series of propylene oxide and spur resin. Next, the cubes were baked at 70 °C from 8 to 10 h. The baked cubes were cut by an ultra-microtome. The pieces with a thickness of 60–90 nm were pasted onto copper grid and stained with uranyl acetate and lead citrate to increase the contrast. The prepared specimens were observed using TEM (JEOL, JEM-2100, Tokyo, Japan).

FISH with 16S rRNA-targeted oligonucleotide probes Two milliliter of mixed liquor suspended solids was fixed in a 4% paraformaldehyde solution for 12 h. Fixed samples were brought into hybridization by following which procedure described elsewhere (Amann et al. 1995). In brief, 10 µL of 16S rRNA-targeted oligonucleotide probe (Table 1) in hybridization

Table 1 Oligonucleotide probes for analyzing microorganisms in nitrifying sludge

Probe	Sequence (5′ to 3′)	Label	Target organisms	Formamide (%)
Nso190	CGATCCCCTGCTTT TCTCC	AF	Many but not all ammonia oxidizing β-Proteobacteria	55
Ntspa662	GGAATTCCGCGCTC CTCT	Cy3	*Nitrospira* genus	35
Nit3	CCTGTGCTCCATGC TCCG	Cy3	*Nitrobacter* spp.	40

buffer was added onto each spot of the samples on microscopic slide. The slides were hybridized at 46 °C for 2 h and washed at 48 °C for 15 min. Later, DNA of all microorganisms in the sample were stained with 0.9 μM DAPI for 15 min. The hybridized samples were then observed under CLSM (FluoView FV10i, Olympus, Japan). With a helping of image analysis software (ImageJ 1.4.3.67, Broken Symmetry Software), the 22 corresponding fluorescence in situ hybridization (FISH)-CLSM images were determined the percent abundance of target microbes in total microbes via estimating an area occupied by microbes being hybridized with the targeted probe per one occupied by DAPI-stained microbes.

Live/dead cell observation The live and dead cells of nitrifying sludge culture taken from the AgNPs and Ag⁺-exposed tests were determined using a staining kit (LIVE/DEAD® BacLight™ Bacterial Viability, Molecular Probes, Invitrogen) and observed under CLSM (FluoView FV10i, Olympus, Japan) (Choi et al. 2008). Live and dead cells were investigated by staining cells with an appropriate mixture of the SYTO 9 and propidium iodide (PI) stains according to the manufacturer's protocol. All bacterial cells were stained with fluorescent green from SYTO 9 whereas dead cells (damaged cells) were only stained with fluorescent red from PI. The presence of dead cells would reduce the emission of fluorescent green. The autoclaved nitrifying sludge was used as a positive control for the dead cells. The excitation/emission maxima for SYTO 9 and PI stains were 480/500 and 490/635 nm, respectively. At least ten images from CLSM of each sample were used for calculation of the areas of live and dead cells using the software ImageJ (Gu et al. 2014).

Results and discussion

Inhibitory mechanism and kinetics of ammonia oxidation

The ammonia oxidation experiments with and without AgNPs were performed. The ammonia concentrations depleted with time in all of the experiments. The rates of ammonia reduction were used to fit the Monod model as shown in Fig. 2a. Supplement of AgNP concentrations of 1, 10, and 100 mg/L led to a sharp decrease in K_s and q_{max} (Fig. 2a). The values of K_s

and q_{max} were reduced from 13.49 to 3.72 mg/L and from 0.6982 to 0.1128 mg N/L/h when AgNP concentrations increased from 0 to 100 mg/L, respectively. The ammonia oxidation activity was inhibited by 50.5 ± 9.48, 63.3 ± 7.9, and $76.8 \pm 5.8\%$ at the AgNP concentration of 1, 10, and 100 mg/L, respectively (Fig. 3a). It is noted that in order to mimic toxicity of silver in environment, the synthetic wastewater with several salts including chloride ions was used. Silver ion could form certain portions of AgCl affecting toxicity of Ag⁺. Based on estimation of silver species in SWW using visual MINTEQ (version 3.0), Ag⁺ and AgCl were major species with total proportion of higher than 80% among aqueous species. According to Choi et al. (2008), AgCl and Ag⁺ inhibited respiration of autotrophic nitrifying microorganisms at the same magnitude (42 and 46%, respectively). Therefore, Ag⁺ may combine with chloride ions but the combination did not necessarily influence the toxicity of Ag⁺ in the experimental solution. Based on the result, it is clear that the initial AgNP concentrations significantly affected the inhibitory magnitude ($p = 0.002$), which was found similar with previous works (Giao et al. 2012; Gu et al. 2014) that higher AgNP concentration resulted in more inhibition of AO. However, the prior studies did not conclude whether the inhibition of ammonia oxidation was mainly from AgNPs themselves or released Ag⁺.

The released Ag⁺ was monitored along with the ammonia oxidation inhibition in AgNP experiments as shown in Table 2. The Ag⁺ concentrations were measured from the experiments with SWW and SWW+NS (the wastewater with the nitrifying sludge) at different initial ammonia and AgNP concentrations. There was more released Ag⁺ at higher initial AgNP concentrations. This could be the result of an instant dissociation of Ag⁺ from AgNPs or the stock AgNPs previously contained Ag⁺ since concentration of Ag⁺ release was detected immediately after AgNPs were added to SWW or SWW+NS. Prior studies found that concentration of dissolved silver increased sharply in a short time after AgNPs were added to the medium (Lee et al. 2012; Yuan et al. 2013). The increasing Ag⁺ concentration with time (from 0 to 30 h) was obviously indicated that AgNPs could gradually release Ag⁺ after they are in WWTPs. The finding agreed with other studies reporting that AgNPs were the source of Ag⁺ (Lee et al. 2012; Massarsky et al. 2014) because they produce peroxide intermediates (H_2O_2), which oxidize metal silver to Ag⁺
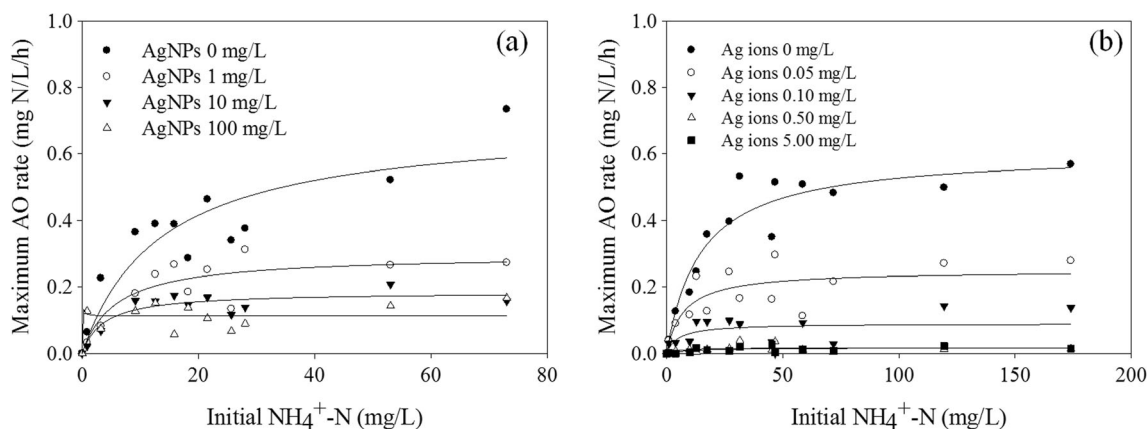
Fig. 2 Kinetics of AO from nitrifying sludge with **a** AgNPs and **b** Ag$^+$

(Liu and Hurt 2010). In this study, the concentrations of Ag$^+$ reduced from 30 to 60 h. The possible explanation for the reduction of Ag$^+$ release was due to binding to inorganic ligand such as chloride (Choi et al. 2009; Yang et al. 2014). In addition, Ag$^+$ can strongly combine with thiol groups found in biomass (Gordon et al. 2010; Morones et al. 2005).

The initial AgNP concentrations at 1, 10, and 100 mg/L released the average amounts of Ag$^+$ of 0.059, 0.171, and 0.503 mg/L in SWW after 60 h of experimental period. These ranges of concentrations were chosen for the inhibitory kinetic experiment. The ammonia reduction rates under the presence of Ag$^+$ were used to fit Monod model as shown in Fig. 2b. Similar to AgNPs, amendment of Ag$^+$ into nitrifying culture resulted in a rapid decrease in K_s and q_{max} (Fig. 2b). An increasing addition of Ag$^+$ concentrations from 0 to 0.50 mg/L resulted in a decrease of K_s and q_{max} from 17.83 to 4.76 mg/L and from 0.6379 to 0.0175 mg N/L/h, respectively. It was observed that q_{max} values were similar (0.0175 mg N/L/h) at Ag$^+$ concentrations of 0.50 and 5.00 mg/L (Fig. 2b). For the AO activity, Ag$^+$ at 0.05, 0.10, 0.50, and 5.00 mg/L suppressed AO by 52.7 ± 2.1, 75.3 ± 1.8, 93.9 ± 1.9, and $96.2 \pm 1.3\%$, respectively (Fig. 3b). It was

clear that the released Ag$^+$, which was at very low concentrations, resulted in high inhibition of AO. Former studies reported that the Ag$^+$ played role in causing toxic inhibition for *Nitrosomonas europaea* (Arnaout and Gunsch 2012; Radniecki et al. 2011). Therefore, this study confirmed that the toxicity of AgNPs should be mainly from the role of Ag$^+$ release.

Previous studies also demonstrated that the toxicity of Ag$^+$ was higher than AgNPs to several types of organisms. The potential nitrification of both *N. europaea* biofilms and free cells was more adversely impacted by toxicity of Ag$^+$ than AgNPs (Barker 2014). Similarly, toxicity of Ag$^+$ to *Daphnia magna* and *Thamnocephalus platyurus* was also found higher than that of AgNPs (Blinova et al. 2013). Higher toxicity of Ag$^+$ was because Ag$^+$ could produce more ROS (Gu et al. 2014), easily uptaken by ion transporters and high affinity to thiol groups (Gordon et al. 2010), thus exhibiting more toxic impact than AgNPs. The inhibitory constants, K_i values, supported the evidence that Ag$^+$ was more toxic to AO activity than AgNPs. It was found that the K_i of Ag$^+$ was much lower (0.29 mg/L) than that of AgNPs (73.5 mg/L) in the current study. The Monod kinetic parameters including K_s and q_{max}
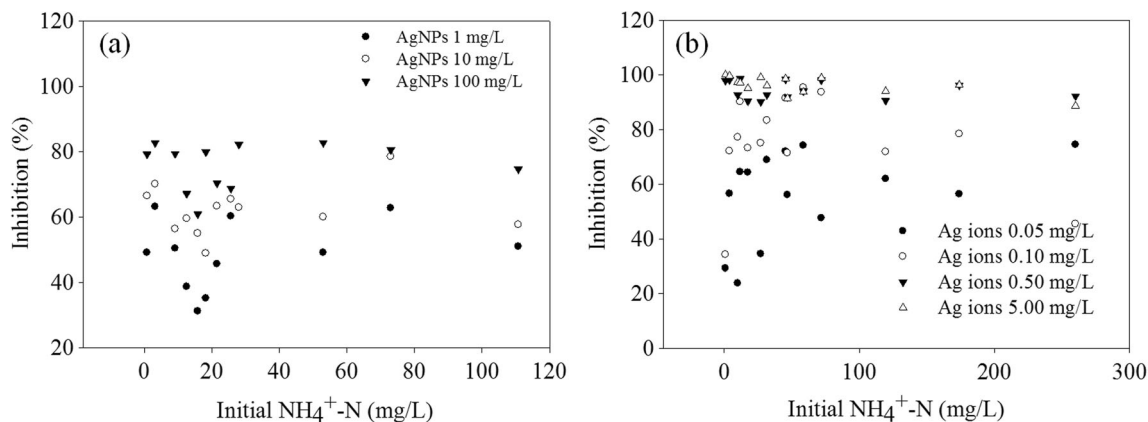

Fig. 3 Percent inhibition of AO from nitrifying sludge by **a** AgNPs and **b** Ag$^+$

Table 2 Concentration of Ag$^+$ release from AgNPs

Initial NH$_4^+$–N (mg/L)	Type of medium	Initial AgNPs (mg/L)	Ag ion release from AgNPs (μg/L)		
			Mean ± SD		
			0 h	30 h	60 h
0	SWW only	1	71.7 ± 7.6	80.0 ± 10.0	25.3 ± 0.6
0	SWW only	10	77.6 ± 10.0	232.9 ± 2.9	202.4 ± 32.1
0	SWW only	100	227.2 ± 15.3	750.9 ± 20.8	529.6 ± 10.4
20	SWW + NS	1	4.0 ± 0.1	< DL	< DL
20	SWW + NS	10	< DL	< DL	12.8 ± 7.5
20	SWW + NS	100	180.9 ± 15.3	280.2 ± 36.1	211.4 ± 12.6
100	SWW + NS	1	18.0 ± 3.2	< DL	< DL
100	SWW + NS	10	< DL	< DL	< DL
100	SWW + NS	100	135.6 ± 20.0	578.4 ± 8.4	331.4 ± 0.0

DL detection limit, <3 μg Ag/L

showed that the inhibitory effect of AgNPs and Ag$^+$ on the AO activity from nitrifying sludge followed uncompetitive-like model because both K_s and q_{max} decreased when the concentrations of AgNPs and Ag$^+$ increased. Our previous study also found that AgNPs inhibited AO process best described by uncompetitive-like model (Giao et al. 2012)
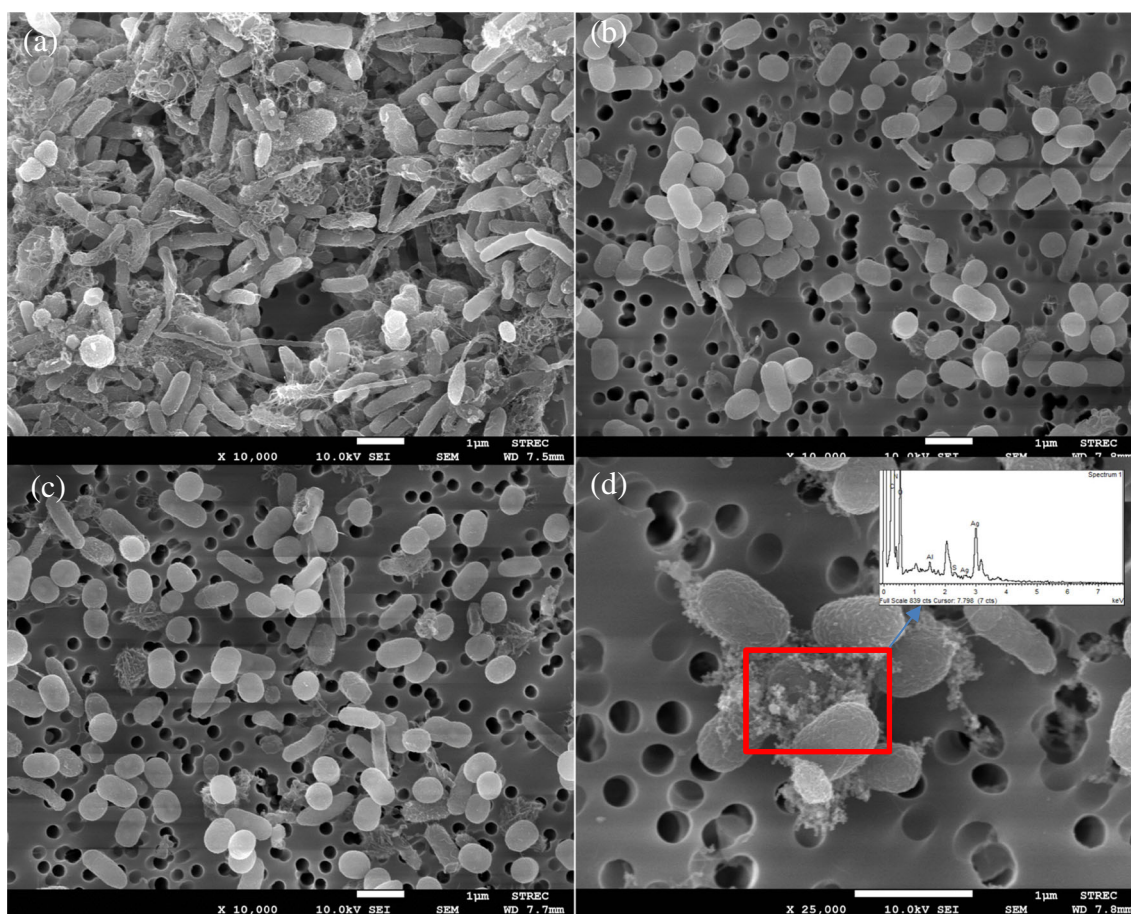

Fig. 4 SEM micrographs for observation of nitrifying sludge after 48 h exposed to AgNPs and Ag$^+$. **a** SEM image for the control (without AgNPs or Ag$^+$). In the control, microbes were in rod-shaped and filamentous observed at the magnification of ×10,000. **b** Microbes in the nitrifying sludge became a shorter rod-shaped after exposing to AgNPs at 10 mg/L observed at ×10,000. **c** Microbes in nitrifying sludge have changed to shorter rod-shaped after exposure to Ag$^+$ at 0.10 mg/L observed at ×10,000. **d** AgNP particles exposed and formed aggregates with cells observed at the magnification of ×25,000
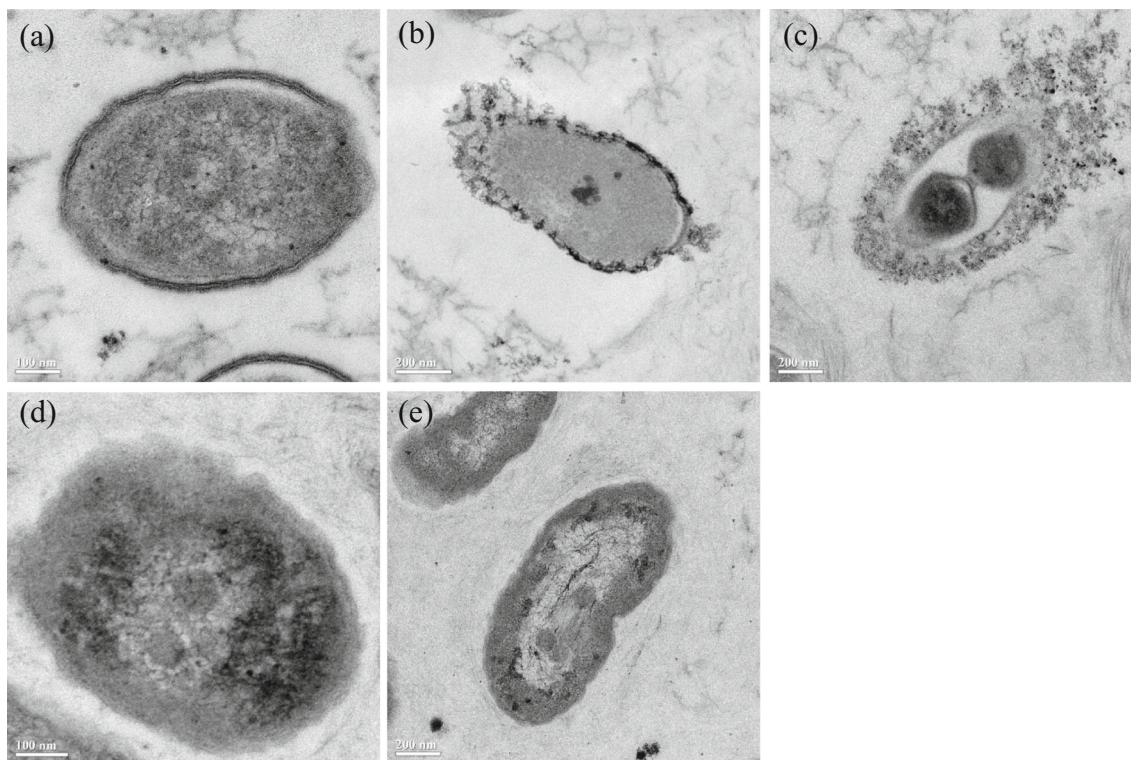
Fig. 5 TEM images of nitrifying sludge after 48 h exposed to AgNPs and Ag⁺: **a** the control without silver, **b** AgNPs 10 mg/L, **c** AgNPs 100 mg/L, **d** Ag⁺ 0.10 mg/L, and **e** Ag⁺ 0.50 mg/L. AgNPs attached on the surface and caused damage of cell in the samples treated with AgNPs. Cells treated with Ag⁺ had less-defined membrane, and the internal parts of the cells formed vesicles indicated by a lighter in color compared to the control

although the oxygen uptake rates were measured instead of ammonium.

It was noticed that AgNP concentrations of 1, 10, and 100 mg/L inhibited AO by 50.5 ± 9.5, 63.3 ± 7.9, and $76.8 \pm 5.8\%$, respectively, while Ag⁺ (similar to Ag⁺ released from AgNPs) at 0.05, 0.10, and 0.50 mg/L suppressed AO by 52.7 ± 2.1, 75.3 ± 1.8, and $93.9 \pm 1.9\%$, respectively (Fig. 3). The inhibitory effect of AgNPs suspension (from AgNPs themselves, released Ag⁺, and ROS) in these inhibitory experiments should have been similar or higher than that influenced by Ag⁺ (at equal concentration to the released amount) using AgNO₃ as Ag⁺ source. However, from the experiment, AgNPs suspension showed apparent lower inhibitory effect on AO compared to that of Ag⁺ using AgNO₃ as Ag⁺ source in the inhibitory test. This could be due to two potential reasons. Firstly, AgNPs gradually liberated Ag⁺ and some factors (such as inorganic ligand, thiol groups) reduced Ag⁺ under the presence of biomass. This can be seen from the Ag⁺ release in SWW+NS, which was much lower than in SWW due to the presence of nitrifying biomass (Table 2). The reduction of released Ag⁺ could lead to lower initial Ag⁺ concentrations in AgNP experiment compared to those in Ag⁺ experiment (AgNO₃ as a Ag⁺ source). As a result, lower toxicity to AO was observed in AgNPs experiment. In addition, Ag⁺ possibly exhibited acute toxic effect on AO. It might take time for

AgNPs to release Ag⁺ to a level similar to direct Ag⁺ from AgNO₃. During slow Ag⁺ releasing period, ammonia oxidizers could gradually adapt to the environment. Similarly, Gu et al. (2014) reported that the oxygen uptake rate of flocculent sludge was inhibited in the short-term test (12 h) but the inhibition was absent during the long-term exposure (22 days) to AgNPs at 50 mg/L due to adaptation of the microbes in the sludge. In addition, AgNPs themselves could aggregate or bind to the nitrifying sludge led to formation of larger sizes of particles. Prior studies demonstrated that AgNPs with larger sizes dissociated less Ag⁺ (Li et al. 2015) and poorer interacted with cells (Radniecki et al. 2011) thus reducing their toxicity. In this study, the release of Ag⁺ in the AgNPs experiment and the toxicity of Ag⁺ in the kinetics test suggested that Ag⁺ released from AgNPs mainly contributed to overall toxicity of AgNPs.

Microbial cell physiology observation

The microbial cell physiology of the nitrifying sludge exposed to AgNPs and Ag⁺ observed by SEM and TEM was shown in Figs. 4 and 5. The introduction of AgNPs into the nitrifying sludge resulted in AgNP–cell aggregation, which was confirmed by the EDX image (Fig. 4d, inset). Comparing to the control (Fig. 4a), it is likely that major microbial population in
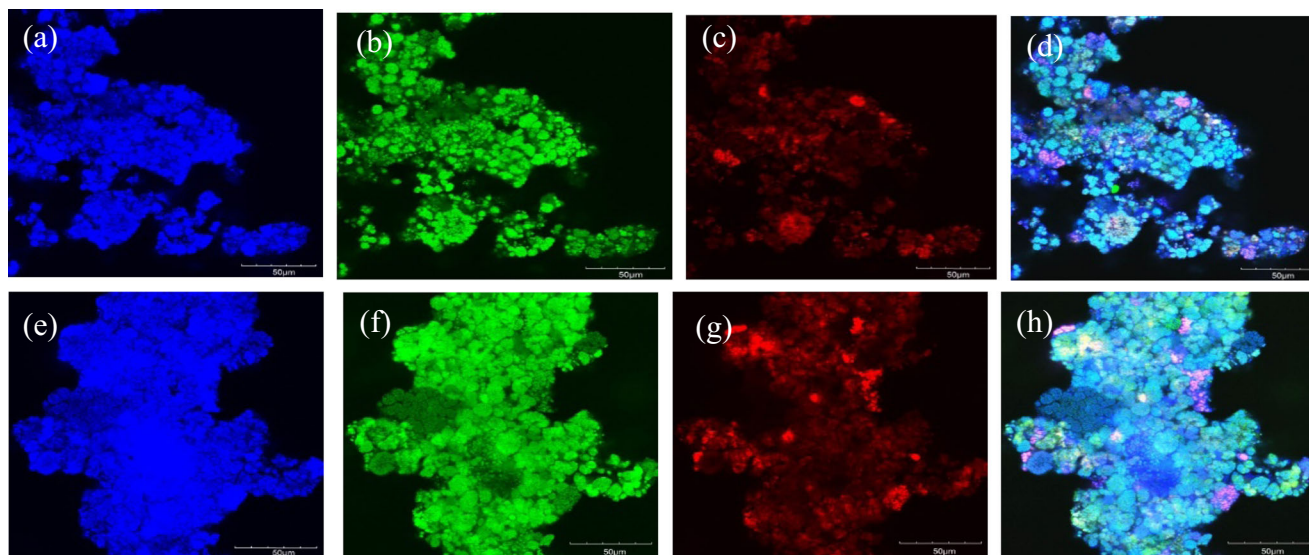
Fig. 6 Example of FISH-CLSM images of microbes in nitrifying sludge. Total microorganisms were DAPI stained (*blue*), AOB was hybridized with NSO190 (*green*), *Nitrobacter* sp. was hybridized with Ntspa 662 (*red*), and *Nitrospira* sp. was hybridized with NIT3 (*red*). The target cells combine with both Alexa Flour 488-labeled probe (in *green*) and CY3-labled probe (in *red*), were in *yellow*. The percent abundance of target microbes in total microbes was determined by estimation of an area occupied by microbes being hybridized with the targeted probe per one occupied by DAPI-stained microbes. FISH signal of total microorganisms is shown in **a** and **e**, whereas AOB was indicated in **b** and **f**. *Nitrobacter* sp. and *Nitrospira* sp. were presented in **c** and **g**, respectively. Combination of FISH signals of all microorganisms, AOB and *Nitrobacter* sp. was illustrated in **d** while combination of all microorganisms, AOB and *Nitrospira* sp. was showed in **h**

the samples amended with AgNPs at 10 mg/L or Ag^+ at 0.10 mg/L looked shorter (Fig. 4b, c). Chakravarty et al. (2007) used copper ions (Cu^{2+}) to expose to *Acidocella* sp. GS19h strain; the observed morphological change of the cells was similar to the current study. Morphological changes are the way that several bacteria used to adapt themselves during the presence of heavy metals (Chakravarty et al. 2007). The morphological change was due to the relative reduction of cell surface (due to cell membrane reduction) with respect to the cell volume. The reduction of cell surface enabled microbes to become less exposed to heavy metals (Chakravarty et al. 2007). In this study, the microorganisms in the nitrifying sludge were the mixed cultures. It could be possible that the cells in the nitrifying sludge changed their morphology as a response to the stressful condition resulted from AgNPs and Ag^+ or predominant bacteria in microbial community changed. The continued work on microbial change issue should be performed.

In the present study, TEM results indicated that AgNPs attached on outer layer of the cells, formed pits and damaged cell membrane (Fig. 5b, c). After the attachment, AgNPs sloughed off the outer layer and caused cell death resulting in the reduction of AO in nitrifying sludge. In addition, the released Ag^+ from AgNPs could cause additional toxicity to the cells as discussed earlier. Damage of bacterial cell membrane caused by AgNPs was previously reported in the literatures (Choi et al. 2008; Giao et al. 2012; Siripattanakul-

Ratpukdi et al. 2014). Besides, Ag^+ could enhance toxicity of AgNPs via binding to the membrane surface and inactivating the activity of the functional enzyme of ammonia oxidizers (Arnaout and Gunsch 2012).

The binding of AgNPs and Ag^+ on the cell surface resulted in the damage of cell wall. Moreover, the interior cells after exposing to Ag^+ (Fig. 5d, e) were different from no silver control (Fig. 5a). The area of lighter color of the samples treated with Ag^+ was more intense than in the control. The finding in this study agreed with the previous study reporting that bacteria responded to silver stress by forming vesicles resulting in less density of internal parts of the cell treated with Ag^+ (Arnaout and Gunsch 2012). This could be the reason to explain cells change from rod-shaped to shorter rod-shaped in the previous discussion of SEM. TEM observation also indicated that the outer layer of the cell exposed to Ag^+ was thinner than that of the cell without exposing to silver, which could be from the Ag^+ interfering with peptidoglycan layer and cytoplasmic membrane (Jung et al. 2008). The loss of defined membrane could then lead to cell death, and loss of AO activity. The less-defined membrane in cells exposed to Ag^+ than those exposed to AgNPs could be the reason for the more toxic impact of Ag^+ than AgNPs. The changes of cell morphology, density of internal cell matters, defined membrane, and cell damages were well linked to the inhibitory effect of AgNPs and Ag^+ on AO activity as discussed in earlier section.
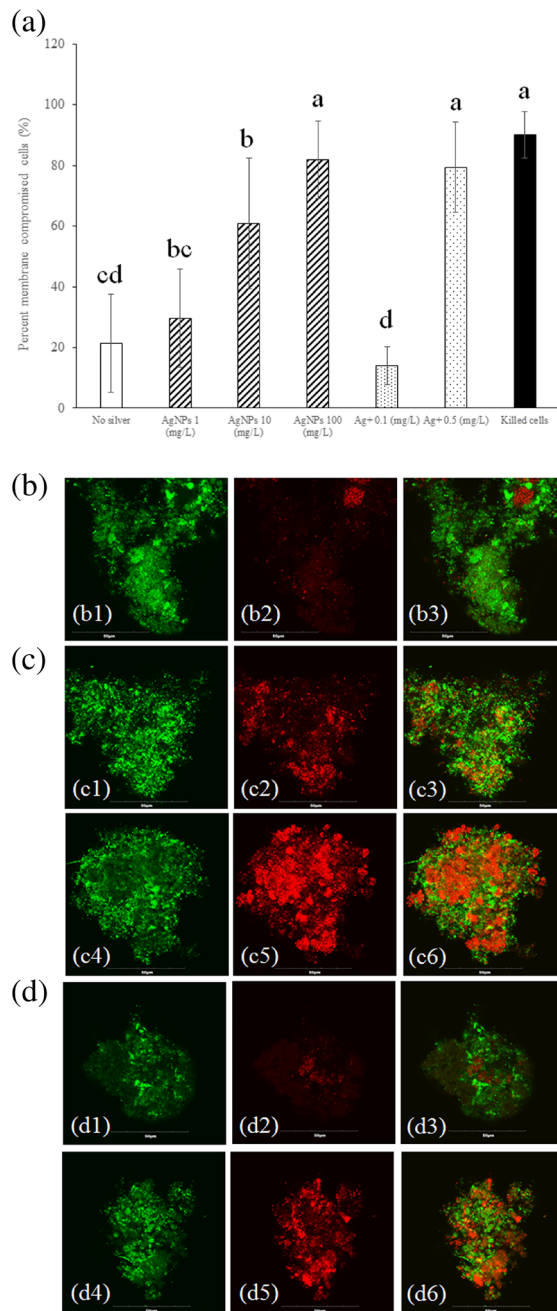
(a)

Microbial community and viability observation

Estimation from FISH-CLSM images (Fig. 6) indicated that AOB were mostly dominant in nitrifying culture ($59.0 \pm 10.0\%$ of total microbes). While the nitrite-oxidizing bacteria (NOB) including *Nitrospira* sp. and *Nitrobacter* sp. accounted for 4.9 ± 4.0 and $22.8 \pm 5.7\%$ of total microbes, respectively. The results clearly indicated that ammonia-oxidizing culture was dominant in the nitrifying sludge. This was well fitted to the previous discussion that obvious inhibition of AO from the nitrifying culture in the inhibitory kinetics experiments with AgNPs and Ag^+ was found.

Since the majority of microbes found in this study was AOB and NOB, the bacterial viability test was performed (Fig. 7). The percent damage of cell membrane resulted from exposure to AgNPs and Ag^+ was showed in Fig. 7a and example of CLSM images of membrane integrity of bacterial cells influenced by AgNPs and Ag^+ was provided in Fig. 7b–d. According to Fig. 7a, the damage of membrane integrity of bacterial cells treated with AgNP concentrations at 1, 10, and 100 mg/L accounted for 29.7 ± 16.2, 60.9 ± 21.6, and $81.8 \pm 12.8\%$, respectively. While bacterial cells amended with Ag^+ at 0.10 and 0.50 mg/L resulted in membrane integrity loss by 14.1 ± 6.3 and $79.5 \pm 15.0\%$, respectively. It is clearly that Ag^+ at 0.50 mg/L caused loss of membrane integrity as high as that of AgNPs at 100 mg/L, which reaffirmed the previous finding that Ag^+ was more toxic to AO than AgNPs. In addition, the increasing percentage of dead cells agreed with the increasing inhibition magnitude of AO when AgNPs and Ag^+ concentrations increased. However, damage of membrane integrity was not significantly different ($p < 0.05$) between the silver control, AgNPs at 1 mg/L and Ag^+ at 0.10 mg/L (Fig. 7a). This was not expected since AgNPs and Ag^+ at these concentrations significantly inhibited AO by 50.5 ± 9.48 and $52.7 \pm 2.1\%$, respectively. It was possible AgNPs and Ag^+ at these low concentrations could partially cause damage of membrane integrity, but the damage was not detected based on our investigation using ten live/dead images. However, prior study reported that cell lysis was only partial reason for the inhibition of nitrification of AgNPs and Ag^+ (Barker 2014). In addition, former studies indicated that Ag^+ could inhibit functional enzymes, thus reducing AO without completely destroying the cell membrane (Arnaout and Gunsch 2012; Gu et al. 2014).

In this study, SEM images indicated that AgNPs attached on the microbial cells while TEM results revealed that AgNPs and Ag^+ reduced thickness of outer layer and damaged bacterial cells. In addition, live/dead assay confirmed that AgNPs and Ag^+ damaged membrane integrity. Previous study also found that AgNPs and Ag^+ generated reactive oxygen species (ROS) and then ROS caused damage of cell wall (Arnaout and Gunsch 2012; Hwang et al. 2008; Sharma et al. 2009; Yuan et al. 2013), formed pits (Siripattanakul-Ratpukdi et al. 2014)

(b)
(c)
(d)

Fig. 7 Percent of cell membrane damaged by AgNPs and Ag^+ after 48 h of exposure (**a**). The average percentage of live/dead results were calculated based on ten CLSM images. *Error bars* represent the standard deviation. *Different letters* indicate statistically significant ($p < 0.05$). Example of CLSM images of membrane integrity of bacterial cells under control (**b**), AgNPs (**c**), and Ag^+ (**d**) condition after 48 h of exposure. *b1*, *b2*, and *b3* showing the total cells, dead cells, and overlay of total and dead cells for the control; *c1*, *c2*, and *c3* showing the total cells, dead cells, and overlay of total and dead cells for the sludge exposed to AgNPs 10 mg/L; *c4*, *c5*, and *c6* showing the total cells, dead cells, and overlay of total and dead cells for the sludge exposed to AgNPs 100 mg/L; *d1*, *d2*, and *d3* showing the total cells, dead cells, and overlay of total and dead cells the sludge exposed to Ag^+ 0.1 mg/L; *d4*, *d5*, and *d6* showing the total cells, dead cells, and overlay of total and dead cells for the sludge exposed to Ag^+ 0.5 mg/L

resulting in cell death. Our findings agreed with the previously reported results that AgNPs and Ag$^+$ reduced AO by the mechanism of causing cell death.

Conclusion

Amendment of AgNPs and Ag$^+$ into wastewater adversely inhibited the AO process. Silver ions were much more toxic to AO than AgNPs. Silver ions of 0.05 to 0.50 mg/L could inhibit AO by 53–94% whereas AgNPs of 1 to 100 mg/L only reduced AO by 45–74%. Silver nanoparticles released the average amounts of Ag$^+$ at 0.059, 0.171, and 0.503 mg/L over 60-h experimental period at initial AgNP concentrations of 1, 10, and 100 mg/L, respectively. The release of Ag$^+$ mainly caused toxic impact of AgNPs on AO of nitrifying sludge. Microscopic observation indicated that AgNPs attached to microbial cell surfaces and resulted in morphological change. Microbial cells exposed to AgNPs and Ag$^+$ showed less defined membrane and less density of internal cell matters, which could lead to cell death. The result from this study can be used as basic information for preventing the system failure from AgNPs and the released Ag$^+$ by taking relevant pretreatment measures.

Compliance with ethical standards

Conflict of interest The authors declare that they have no conflict of interest.

References

Ahrari F, Eslami N, Rajabi O, Ghazvini K, Barati S (2015) The antimicrobial sensitivity of Streptococcus mutans and Streptococcus sangius to colloidal solutions of different nanoparticles applied as mouthwashes. Dental Research Journal 12:44–49

Amann R, Ludwig W, Schleifer KH (1995) Phylogenetic identification and in situ detection of individual microbial cells without cultivation. Microbiol Rev 59:143–169

APHA (1998) Standard methods for the examination of water and wastewater, 20th edn. American Public Health Association, Washington DC, USA

Arnaout CL, Gunsch CK (2012) Impacts of silver nanoparticle coating on the nitrification potential of Nitrosomonas europaea. Environ Sci Technol 46:5387–5395

Barker LK (2014) Effects of silver ions and nanoparticles on suspended cells and biofilms of Nitrosomonas europaea. Master thesis. University of Oregon State, Corvallis

Beer C, Foldbjerg R, Hayashi Y, Sutherland DS, Autrup H (2012) Toxicity of silver nanoparticles - nanoparticle or silver ion? Toxicol Lett 208:286–292

Blinova I et al (2013) Toxicity of two types of silver nanoparticles to aquatic crustaceans Daphnia magna and Thamnocephalus platyurus. Environ Sci Pollut Res 20:3456–3463

Bower CE, Holm-Hansen T (1980) A salicylate-hypochlorite method for determining ammonia in seawater. Fishery and Aquaculture Science 37:794–798

Chakravarty R, Manna S, Ghosh AK, Banerjee PC (2007) Morphological changes in an Acidocella strain in response to heavy metal stress. Res J Microbiol 2:742–748

Choi O, Deng KK, Kim NJ, Ross J, Surampallie RY, Hua Z (2008) The inhibitory effects of silver nanoparticles, silver ions, and silver chloride colloids on microbial growth. J Water Res 42:3066–3074

Choi O, Clevenger TE, Deng B, Surampalli RY, Ross JL, Hu Z (2009) Role of sulfide and ligand strengh in controlling nanosilver toxicity. Water Res 43:1879–1886

Giao NT, Limpiyakorn T, Siripattanakul-Ratpukdi S (2012) Inhibition kinetics of ammonia oxidation influenced by silver nanoparticles. Water Air Soil Pollution 223:5197–5203

Gordon O et al (2010) Silver coordination polymers for prevention of implant infection:thiol interaction, impact on respiratory chain enzymes, andhydroxyl radical induction. Antimicrob Agents Chemother 54:4208–4218

Gu L, Li Q, Quan X, Cen Y, Jiang X (2014) Comparison of nanosilver removal by flocculent and granular sludge and short- and long-term inhibition impacts. Water Res 58:62–70

Hwang ET, Lee JH, Chae YJ, Kim YS, Kim BC, Sang B, Gu MB (2008) Analysis of the toxic mode of action of silver nanoparticles using stress-specific bioluminescent bacteria. Small 4:746–750

Jung WK, Koo HC, Kim KW, Shin S, Kim SH, Park YH (2008) Antibacterial activity and mechanism of action of the silver ion in Staphylococcus aureus and Escherichia coli. Appl Environ Microbiol 74:2171–2178

Lee Y-J, Kim J, Oh J, Bae S, Lee S, Hong IS, Kim S-H (2012) Ion-release kinetics and ecotoxicity effects of silver nanoparticles. Environ Toxicol Chem 31:155–159

Li L, Wu H, Ji C, van Gestel CAM, Allen HE, Peijnenburg WJGM (2015) A metabolic study on the responses of daphnia magna exposed to silver nitrate and coated silver nanoparticles. Ecotoxicol Environ Saf 119:66–73

Liu J, Hurt RH (2010) Ion release kinetics and particle persistence in aqueous nano-silver colloids. Environ Sci Technol 44:2169–2175

Massarsky A, Trudeau VL, Moon TW (2014) Predictiong the environmental impact of nanosilver. Environ Toxicol Pharmacol 38:861–873

Morones JR, Elechiguerra JL, Camacho A, Holt K, Kouri JB, Ramirez JT, Yacaman MJ (2005) The bactericidal effect of silver nanoparticles. Journal of Nanotechnology 16:2346–2353

Radniecki TS, Stankus DP, Neigh A, Nason JA, Semprini L (2011) Influence of liberated silver from silver nanoparticles on nitrification inhibition of Nitrosomonas europaea. Chemosphere 85:43–49

Schildkraut DE, Dao PT, Twist JP, Davis AT, Robillard KA (1998) Determination of silver ions at sub microgram-per-liter levels using anodic square-wave stripping voltammetry. Environmental Ecotoxicology and Chemistry 17:642–649

Shafer MM, Overdier JT, Armstong DE (1998) Removal, partitioning, and fate of siver and other metals in wastewater treatment plants and effluent-receiving streams. Environmental Ecotoxicology and Chemistry 17:630–641

Sharma VK, Yngard RA, Lin Y (2009) Silver nanoparticles:green synthesis and their antimicrobial activities. Adv Colloid Interf Sci 145:83–96

Siripattanakul-Ratpukdi S, Fürhacker M (2014) Review: Issues of silver nanoparticles in engineered environmental treatment systems Water Air Soil Pollution 225:1939

Siripattanakul-Ratpukdi S, Ploychankul C, Limpiyakorn T, Vangnai AS, Rongsayamanont C, Khan E (2014) Mitigation of nitrification inhibition by silver nanoparticles using cell entrapment technique. J Nanopart Res 16. doi:10.1007/s11051-013-2218-9

USEPA (2009) Targeted National Sewage Sludge Survey Statistical Analysis Report US Environmental Protection Agency Office of Water (4301T) 1200 Pennsylvania Avenue, NW Washington, DC 20460 EPA-822-R-08-018

Westerhoff PK, Kiser MA, Hristovski K (2013) Nanomaterial removal and transformation during biological wastewater treatment. Environ Eng Sci 30:109–117

Yang Y, Wang J, Xiu Z, Alvarez PJ (2013) Impacts of silver nanoparticles on cellular and transcriptional activity of introgen-cycling bacteria. Environmental Ecotoxicology and Chemistry 32:1488–1494

Yang Y et al (2014) Pyrosequencing reveals higher impact of silver nanoparticles than Ag$^+$ on the microbial community structure of activated sludge. Water Res 48:317–325

Yuan Z, Li J, Cui L, Xu B, Zhang H, Yu C-P (2013) Interaction of silver nanoparticles with pure nitrifying bacteria. Chemosphere 90:1404–1411